

DNA Duplex Cage Structures with Icosahedral Symmetry

N. E. Grayson¹, A. Taormina² and R. Twarock³

^{1,3}*Department of Mathematics and Department of Biology
University of York
York YO10 5DD, U.K.*

²*Department of Mathematical Sciences
University of Durham
Durham DH1 3LE, U.K.*

Abstract

A construction method for duplex cage structures with icosahedral symmetry made out of single-stranded DNA molecules is presented and applied to an icosidodecahedral cage. It is shown via a mixture of analytic and computer techniques that there exist realisations of this graph in terms of two circular DNA molecules. These blueprints for the organisation of a cage structure with a noncrystallographic symmetry may assist in the design of containers made from DNA for applications in nanotechnology.

Keywords: Bionanotechnology; Synthetic DNA cage; Icosahedral Symmetry

1 Introduction

RNA cages are known to occur in certain families of viruses. For example, a proportion of the viral RNA of Parvovirus is packaged within the viral particles in the form of a dodecahedral RNA cage [1], and bacteriophage MS2 is known to package part of its genomic material in the form of a 32-faced polyhedron reminiscent of the buckyball [2, 3]. Remarkably, recent advances in biotechnology provide the necessary tools to engineer cage structures from nucleic acids, and open novel avenues for applications in nanotechnology.

DNA cages with crystallographic symmetry have already been realised experimentally in the shape of a cube [4], a tetrahedron [5], an octahedron [6] or a truncated octahedron [7], and one natural idea is to use such cages for cargo delivery or storage [8]. A systematic, theoretical analysis of DNA cage structures is still lacking, and our motivation here is the hope our mathematical considerations on the organisation of DNA in cages with icosahedral symmetry will aid the design of artificial cages inspired by nature.

¹E-mail: neg100@york.ac.uk

²E-mail: anne.taormina@durham.ac.uk

³E-mail: rt507@york.ac.uk -Corresponding author

Models for dodecahedral cages have been derived in [9, 10]. Since a dodecahedron has trivalent vertices and a small number of faces, the combinatorics involved in solving the DNA organisation problem can be done without computer help. This is no longer the case for a four-coordinated polyhedron with thirty-two faces such as the icosidodecahedron. However, icosidodecahedral cages are of particular interest because their volume per surface ratio is the largest in comparison with dodecahedral and icosahedral cages, making them the more appropriate option among these noncrystallographic cages for applications in which the storage or transportation of a larger cargo is required.

We start by introducing our theoretical construction method in general terms for all polyhedra with icosahedral symmetry in Section 2, and then concentrate on icosidodecahedral cages in Section 3 via an approach that combines symmetry arguments and computer analyses.

2 The general set-up: Orientable embeddings and DNA cage structures

We consider the organisation of circular single-stranded DNA (ssDNA) molecules on cages with icosahedral symmetry as in [3]⁴, such that every edge is met by a strand precisely twice in opposite directions. This rule ensures that two different portions of the strand meeting along an edge may hybridize into a duplex structure with the two strands oriented in opposite 3' to 5' directions along that edge.

From a mathematical point of view, we consider the cage as being a graph G whose nodes are the vertices of the cage, and the connectors are its edges. We then search for *orientable thickened graphs*, which are compact orientable 2-dimensional surfaces constructed out of strips and thickened n -junctions glued together, such that the original graph G is topologically embedded into such thickened graphs as a deformation retract [11, 12]. The boundary curves of these thickened graphs form part of circular ssDNA molecules. The aim of this analysis is to realize the graph in terms of a minimal number of circular strands which visit each edge of the cage twice in opposite directions so that the strand segments may hybridize into double helical structures along the edges.

We present an optimization procedure, which takes the following factors into account.

1. *Initial data:* Assuming the cages are made of polygons with all sides of equal length λ , one can imagine to manufacture ssDNA cages of different sizes and therefore, the number $\nu(\lambda)$ of half-turns in the duplex structure along the edges depends on λ ⁵. Configurations where $\nu(\lambda)$ is odd are modelled as cross-overs in the planar projective views of the polyhedra that we are using for our analysis. We remark that there are about 10.5 base pairs (bp) per helical turn.

⁴dodecahedral, icosahedral, 32-faceted polyhedral.

⁵For viruses observed in vivo, the RNA cages have specific sizes and therefore a well-defined $\nu(\lambda)$.

2. *Thickened n -junctions*: Mechanical stress may be imposed on the overall configuration if junctions with an extra number of twists (helical turns) on the legs of the thickened n -junction are introduced. For example, the thickened 4-junction shown in Fig. 1(a) imposes no stress on the configuration (we name it ‘type A’), whilst the thickened 4-junction appearing in Fig. 1(b) accommodates one single twist (we name it ‘type B’) and imposes stress on the overall configuration unless extra nucleotides are introduced (in the non-basepaired inner part of the junction) that compensate for it.

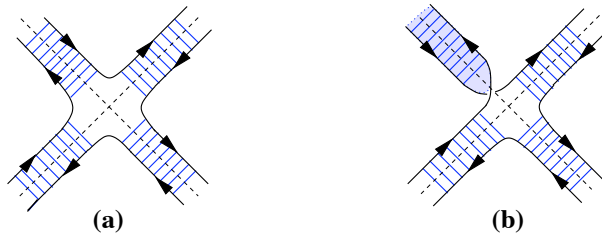


Figure 1: *Thickened 4- junction of type A (a) and of type B (b). The line segments represent base pairs.*

The number n of legs in the junctions depends on the type of cage considered. In Section 3, we consider cages having 4-junctions⁶, but for dodecahedral cages for instance, 3-junctions are needed. In [9], different types of 3-junctions are studied. Apart from those similar to the 4-junctions in Fig. 1, they consider 3-junctions that involve the occurrence of hairpins. We exclude such junctions from our analysis here because they require an extra discussion of how to keep the hairpin in place. In the context of viruses, for example, the protein container acts as a scaffold for the RNA cages. In the context of nanocontainers where such a scaffold is lacking, the hairpin has to be designed such that it interacts with the remaining part of the junction, or, is attached via a sticker strand [14].

The first step in the optimization procedure is to identify *start configurations*, i.e. orientable thickened graphs with a maximum of Type A thickened junctions. Such graphs are usually made of several distinct circular strands that we call *loops*. Our ultimate goal is to construct the graph from a minimal number of such loops, and therefore further junctions need to be replaced in the start configuration to merge loops in a next step.

In order to determine the start configurations, we start by assuming that every vertex on the polyhedron is represented by a type A thickened n -junction. However, in the presence of cross-overs which take into account the odd number of half-turns along the edges, this distribution of type A junctions does not necessarily provide an orientable thickened graph. In particular, this is the case if faces of a cage with an odd number of cross-overs occur.

In this paper, we restrict ourselves to cages which have all edges of the same length, so that the number of helical turns is the same on all edges to start with. Therefore

⁶Four-junctions can be manufactured, see for example [13].

either the strips along these edges are not twisted, i.e. all edges are cross-over free, or the strips are twisted, and all edges have cross-overs, see Fig. 2.

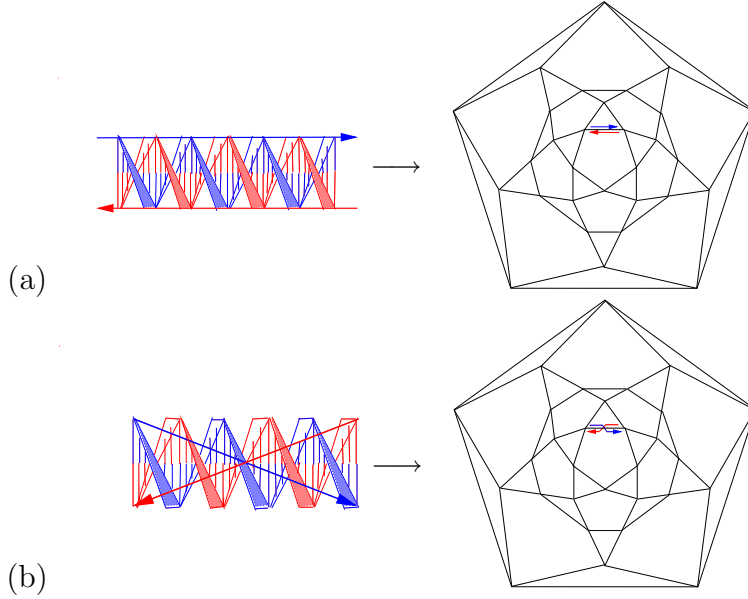


Figure 2: (a) The double helix of DNA is represented by lines (blue and red) that trace the backbone of the helices. (b) Depending on their lengths, additional half-turns may appear, that are represented by cross-overs on the planar representation of the graph.

In the first case, the start configuration is straightforward: All junctions are of type A, and there are as many loops as faces of the polyhedron considered. In the second case where all edges exhibit cross-overs as a consequence of their length, we call *initial data configuration* the 2d surface (orientable or not) obtained by gluing the twisted strips representing the cross-overs to type A thickened n -junctions. **Fig. 3 shows the initial data configuration of the icosidodecahedron. This configuration has twelve loops, but they do not all run in opposite directions so that the initial data configuration does not provide a suitable template for a DNA cage.** In order to decide how many junctions of type B must be introduced in the initial data configuration to obtain a start configuration, we use the notion of *bead* introduced in [10], and follow the *bead rule*. A bead appears on an edge of the polyhedron whenever a twisted strip (cross-over) is glued to the twisted leg of a type B thickened junction, as exemplified in Fig. 4 for a 4-coordinated polyhedron.

The bead rule requires the placement of beads on the edges of the polyhedron such that *all* of the following three conditions are satisfied:

- Each edge accommodates either a cross-over or a bead.
- Every face of the polyhedron in the start configuration must have an *even* number of cross-overs.
- The number of beads is minimal.

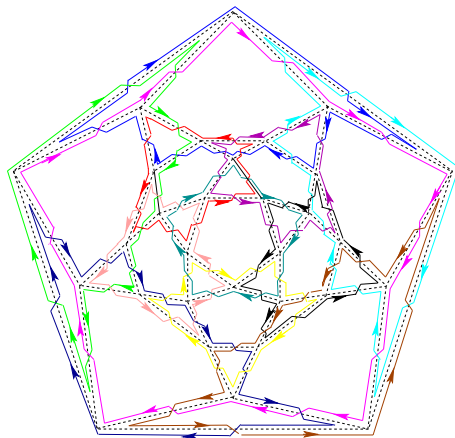


Figure 3: *Initial data configuration for the icosidodecahedron cage when $\nu(\lambda)$ is odd.*

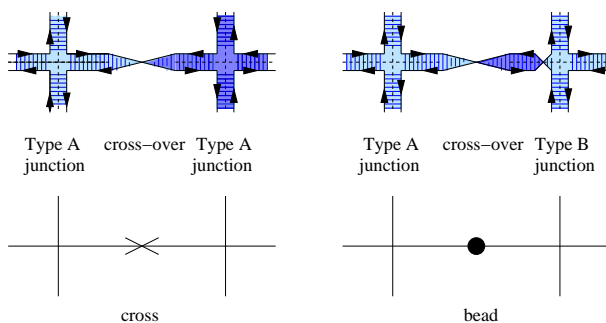


Figure 4: *Emergence of a bead in a modified initial data configuration.*

After the bead rule has been applied, one must identify configurations which are equivalent under icosahedral symmetry. The symmetry-inequivalent bead configurations correspond to the possible start configurations, where some junctions are of type A, and others of type B, the latter having been introduced to provide orientability of the 2d surface.

In order to realize cages via a minimal number of circular DNA molecules, further junctions have to be replaced in the start configuration in order to merge several individual loops into a single loop. We will use the replacement shown in Fig. 5(b), which is the 4-junction analogue to the 3-junction replacement used in [10]. Such a replacement results in the reduction of the overall number of loops (for example in the start configuration) by two. To see this, observe that after replacement the 4-junction is topologically equivalent to two 3-junctions as shown on Fig. 5(c). The upper 3-junction corresponds to Fig. 3 in [10] and, according to this reference, changes the number of loops by two, whilst the lower 3-junction has no effect on the number of loops. The 4-junction replacement thus reduces the number of loops by two. Moreover, note that the upper 3-junction differs from the trivial junction by a few nucleotides only, and hence this 4-junction does not impose stress on the overall cage structure if, as discussed in [10], a few extra nucleotides are introduced at the junctions.

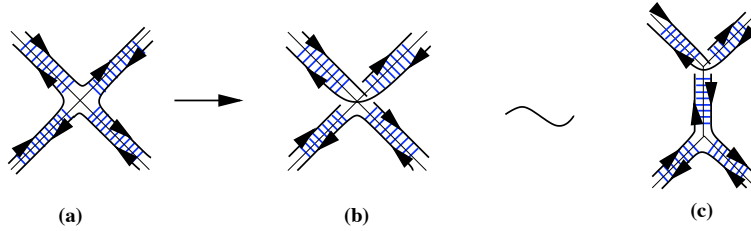


Figure 5: (a) Type A 4-junction, (b) Replacement 4-junction which allows to merge 4 loops into 2, or 3 loops into a single one, (c) The replacement 4-junction is equivalent to two 3-junctions.

3 The example of the icosidodecahedral cage

We consider the 32-faced polyhedron with thirty quaterivalent vertices as an example. Since all edges are of the same length, there are two different scenarios to consider, depending on the sizes of the DNA molecules, see Fig. 2. These scenarios are discussed below.

3.1 Cross-over free cages

In the case where none of the sixty edges of the icosidodecahedral cage has an additional cross-over, as illustrated for one edge in Fig. 2(a), the start configuration consists of thirty-two loops corresponding to the thirty-two faces of the polyhedron, and all 4-junctions (located at the thirty vertices of the cage) are of Type A as in Fig. 5(a). Since every 4-junction replacement in Fig. 5(b) reduces the overall number of loops in the start configuration by two, the minimal number of circular strands needed to realize the cage is two and occurs after fifteen replacements. There is a plethora of different ways of carrying out these replacements in order to arrive at a configuration with only two independent loops L_1 and L_2 , where $L_i, i = 1, 2$ result from merging n_i original start configuration loops, with $n_1 + n_2 = 32$. Extremal cases are (1) $n_1 = 31$ and $n_2 = 1$, i.e. a large loop L_1 combining thirty-one individual loops of the start configuration together with a single loop L_2 from the start configuration that can not be combined with L_1 via the 4-junction replacement of Fig. 5(b), and (2) $n_1 = 15$ and $n_2 = 17$, i.e. two loops of approximately the same size merging fifteen and seventeen loops respectively in the start configuration. An example of the latter situation is presented in Fig. 6. Junctions are represented by circles, while the numbers indicate the order in which 4-junction replacements Fig. 5(b) are carried out. In the case where the 4-junction before replacement hosts four independent loops, the 4-junction replacement leads to the merging of loops corresponding to three of the four faces meeting at this particular vertex, and the arrow indicates the face (and hence the loop) that has not been affected by the replacement. If instead the 4-junction before replacement only hosts three independent loops, the replacement 4-junction merges these three loops in a single one, and no arrow is present. After seven 4-junction replacements, the loops corresponding to all red-shaded faces have been combined into a single loop. Replacements 7 to 15 moreover unite the loops on

all remaining faces into a separate loop that covers all grey-shaded faces. The end result is a template for a duplex cage structure that can be realized by two circular ssDNA molecules.

We end by noting that it is not possible, via the replacement in Fig. 5(b), to create two loops L_1 and L_2 which merge an equal number of original loops in this case, as the topology forces L_1 and L_2 to combine odd numbers of loops from the start configuration.

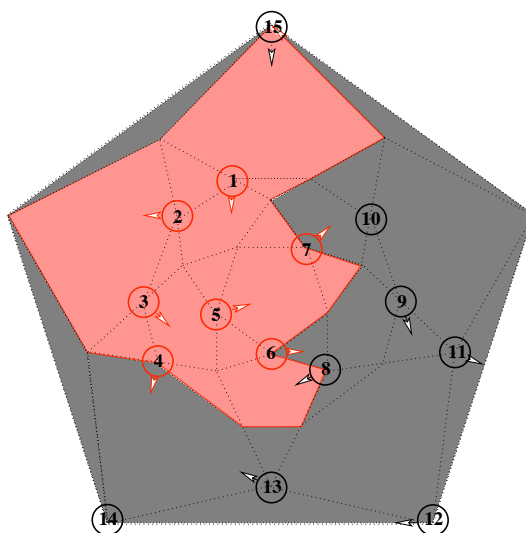


Figure 6: A two strand configuration obtained after fifteen vertex replacements.

3.2 All edges have an additional cross-over.

It may be desirable in an experimental set-up to have a cage structure of a size that requires the occurrence of an additional half-turn on each edge such as in Fig. 2(b), and we therefore also investigate this scenario.

In that case, beads are needed according to the bead rule in order to obtain a start configuration. The minimal number of beads required is easily calculated. All faces of the icosidodecahedron have an odd number of sides: there are twelve pentagons and twenty triangles. Each face must have an even number of cross-overs for orientability. So in particular, each of the twenty triangles must receive at least one bead, but by placing a bead on each triangle, one actually places at least one bead on each pentagon. The distribution of this minimum number of twenty beads should be such that pentagons receive an odd number of beads. Let α be the number of pentagons receiving one bead, β be the number of pentagons receiving three beads and γ be the number of pentagons receiving five beads. Given that there are twelve pentagons in total, we must satisfy the two equations

$$\begin{aligned}\alpha + 3\beta + 5\gamma &= 20, \\ \alpha + \beta + \gamma &= 12,\end{aligned}\tag{3.1}$$

with α, β and γ positive integers. There are three solutions to the problem, namely

$$\begin{aligned}
\text{Case I} & \quad \alpha = 8, \beta = 4, \gamma = 0 \\
\text{Case II} & \quad \alpha = 9, \beta = 2, \gamma = 1 \\
\text{Case III} & \quad \alpha = 10, \beta = 0, \gamma = 2.
\end{aligned} \tag{3.2}$$

We call the three options in (3.2) case I, II and III, respectively, and start by considering case I. This tells us that the bead rule is fulfilled if there are four pentagons with three beads each, and if every triangle has precisely one bead. We therefore determine all symmetry-inequivalent start configurations with that property.

Since this is a significant combinatorial task for the polyhedron under consideration, a purely analytical approach as in [10] is inappropriate here. We therefore adopt a combined analytical/computational approach.

In the first instance, we use the icosahedral symmetry to reduce the number of options to be considered. In particular, we determine all symmetry-inequivalent distributions of four pentagonal faces on the icosidodecahedron. Each of these four faces will then have three of its sides decorated by one bead, whilst all other pentagons and all triangles will have only one bead on their perimeter. In order to determine all inequivalent configurations of four pentagons, we consider the equivalent problem of finding all different possibilities of colouring four of the twelve vertices of an icosahedron.

There are nine inequivalent such configurations for case I, which we call the *partial start configurations*. We show them schematically in a projective view of the icosahedron in Fig. 7.

Inequivalent bead configurations for each partial start configuration: Each partial start configuration encodes several possible cage scenarios which correspond to all inequivalent ways of placing three beads on the sides of four distinguished pentagons, and one bead on one of the sides of all other faces (pentagonal or triangular). We carry out this task computationally.

We have written a computer programme that tests, for each start configuration, which combinations of beads are possible, given the fact that the four distinguished pentagonal faces each have three beads, while all others have one. The results of this programme are encoded as vectors with twenty entries, where each entry represents a triangular face of the icosidodecahedron. The entries are from the set $\{0, 1, 2\}$, and encode which of the three sides contains the bead with respect to our labelling system. In a next step, we translate each such vector into a configuration of loops as follows: we start with an arbitrary edge and, following the rules implied by crosses and beads, continue until we meet the starting point and therefore form a loop. We then choose another starting point and follow the same scenario until the entire graph has been covered in loops, such as in Fig. 3 for example. We then perform a similar analysis for cases II and III.

The results of this approach are summarised in Table 1. In particular, the smallest number of distinct loops is ten and the largest number sixteen. While there are over 10^4 distinct 10-loop configurations, there is only one configuration with sixteen loops, occurring in case III. The vertex configurations involve either four, three, or two distinct loops. We use a computer programme to determine the occurrence

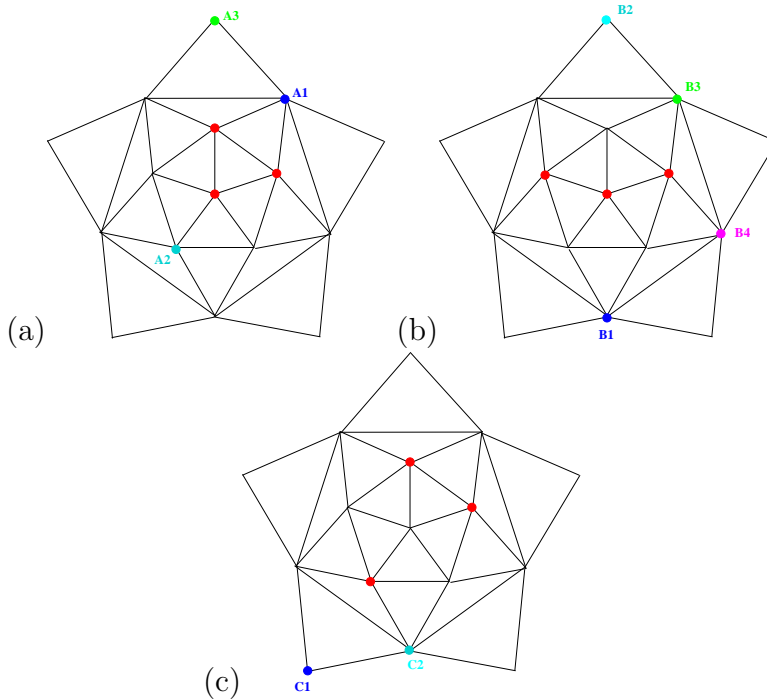


Figure 7: *Partial start configurations for case I, with a distribution of four out of twelve pentagons on the icosidodecahedron, represented here as distributions of four vertices on an icosahedron: (a) configurations with three vertices being those of a triangle (red) and the fourth vertex being either A_1 , A_2 or A_3 ; (b) configurations with three red vertices and the fourth one being either B_1 , B_2 , B_3 or B_4 ; (c) configurations with three red vertices and the fourth one being either C_1 or C_2 .*

of the different vertex types for each start configuration. Remarkably, for all start configurations with ten loops, at most three distinct loops meet at each junction. Since replacements of type Fig. 5(b) reduce the total number of strands by two at each incidence, and hence by an even number in total, the minimal number of loops needed to realise the cage structure via our formalism is two. These two loops could potentially be merged as in [10] by a hairpin construction, but this is not considered here.

Since there is only one start configuration with sixteen loops, we consider this case first: seven replacements are required to reduce the overall number of loops to two, and there are many different ways of achieving this. In Fig. 8 we display one solution that leads to two loops L_1 and L_2 with $n_1 = 7$ and $n_2 = 9$.

Loop number	Case I	Case II	Case III
10	11527	0	0
12	343	951	0
14	3	8	73
16	0	0	1

Table 1: *The distribution of 10-, 12-, 14- and 16-loop start configurations among the three different cases.*

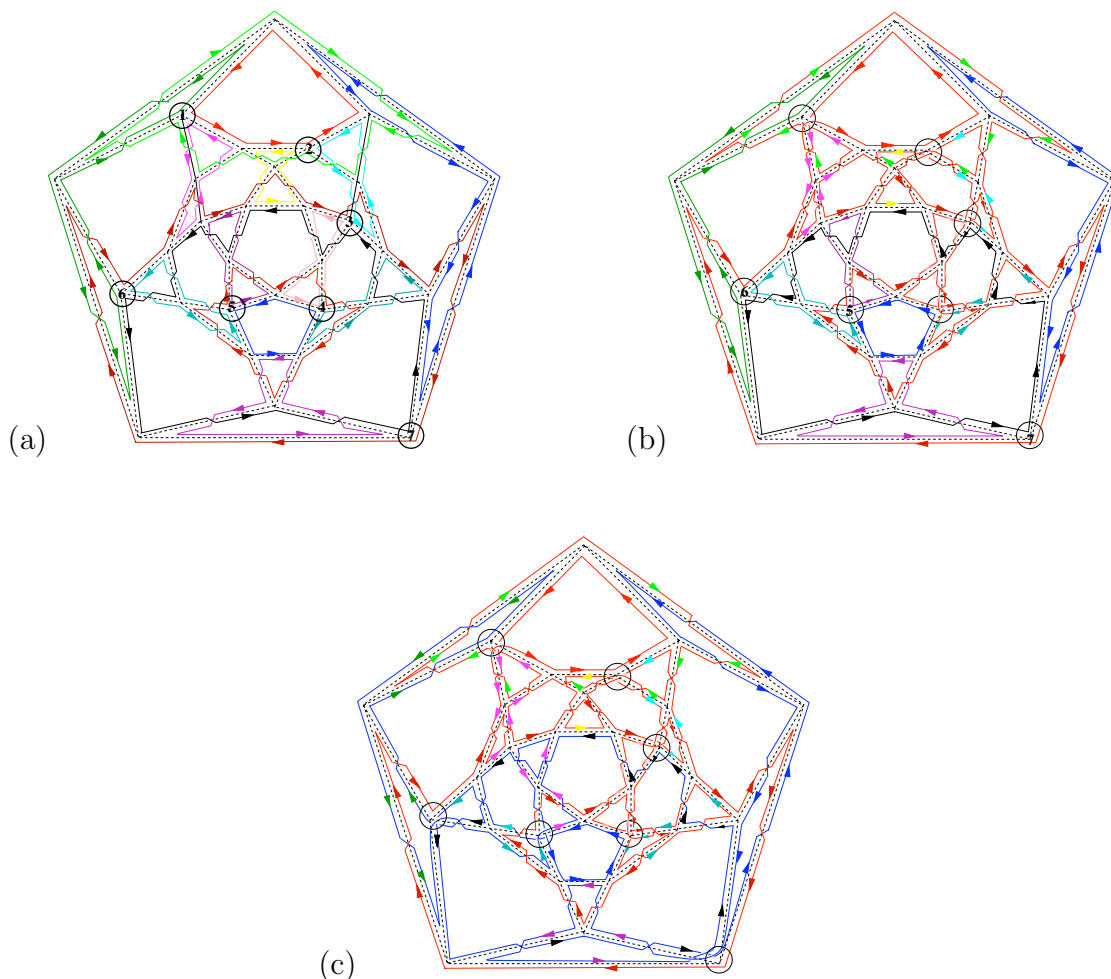


Figure 8: *The 16-loop start configuration with numbered junctions indicating the replacements that lead to two distinct loops obtained from merging seven (resp. nine) starting configuration loops.*

In Fig. 8(a), circles indicate the locations of the junctions at which replacements are taking place and the numbers keep track of the order of replacements by junctions of type Fig. 5(b). Fig. 8(b) shows the result after replacements 1 to 4 have been carried out to merge nine loops into one larger loop (shown in red). Colours of the arrows on the strands indicate the colour of the loop before it has been merged into the larger (red) loop via the 4-junction replacement. Fig. 8(c) presents the resulting configuration in terms of two independent loops, the red one being that of Fig. 8(b)),

and the blue one being obtained after replacements 5 to 7). This provides a template for the realisation of the cage in terms of two circular ssDNA molecules.

Among the start configurations with twelve or fourteen loops, there are various occurrences of vertices with four distinct loops, for example either none or in-between three and seventeen such vertices for the 12-loop configurations, and either none or in-between ten and eighteen such vertices for the 14-loop configurations. As an example we consider the 14-loop configuration in Fig. 9.

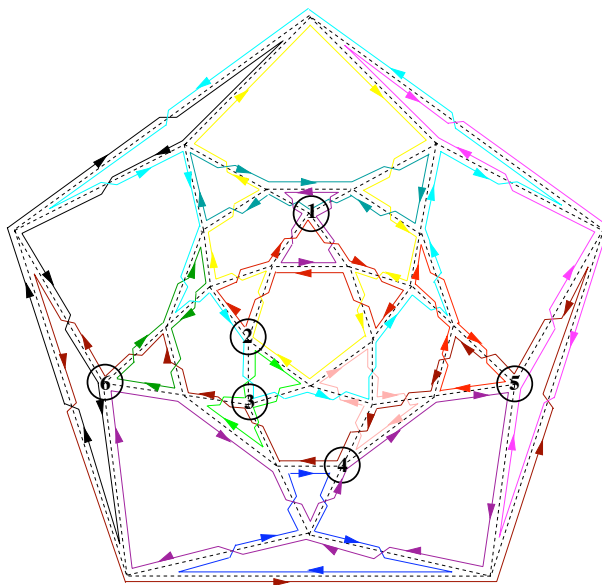


Figure 9: A 14-loop starting configuration with numbered junctions indicating the replacements that lead to two distinct loops obtained from merging seven starting configuration loops each.

In this case, six replacements are necessary to obtain a two-loop configuration. We indicate the locations of six replacements leading to a configuration in terms of two separate loops, each uniting seven loops of the start configuration (i.e L_1 and L_2 with $n_1 = n_2 = 7$). Note that unlike the previous case of a 16-loop start configuration, a 14-loop start configuration can be realised in terms of two loops merging the same number of smaller loops in the start configuration, because 14 is twice an odd number, and loops L_i can only merge odd numbers of starting configuration loops. In general, it is only possible to obtain two loops L_1 and L_2 with $n_1 = n_2$ if the start configuration exhibits $2(2k + 1)$ loops for k integer (and then, $n_1 = n_2 = 2k + 1$). So it is possible for the 10-loop start configurations, but not for any other start configuration corresponding to an entry in Table 1.

The configurations in Fig. 8(c) and Fig. 9 are two examples of cage structures that can be realized via two circular DNA strands. In contrast with the cage in Fig. 6, however, there are extra stresses created by the twists that have been introduced in order to make the structure orientable. These stresses can be compensated in two ways, either by introducing a few additional nucleotides in the non-basepaired middle portion of the junction on the expense of making these junctions slightly less rigid,

or, if rigid junctions are wanted, by adjusting the lengths of the edges accordingly. A given experimental setting or desired application would dictate which of these options is more appropriate.

4 Discussion

We have performed a theoretical analysis of icosidodecahedral cages formed from two circular DNA molecules in a duplex structure. With applications in nanotechnology in mind, emphasis was placed on minimising mechanical stress at the vertex junctions. We have shown that as for the dodecahedral cages considered in [10], there exist realisations of the icosidodecahedral cage in terms of two DNA molecules. However, the icosidodecahedral cages considered here have a larger volume per surface ratio than the dodecahedral cages and may therefore be more suitable for nanotechnology applications in which the cages serve as containers for storage or the transport of a cargo.

Various types of crystallographic cages have been realised before, and we hope that the blueprints for the organisation of icosidodecahedral cages suggested here may assist in their experimental realisation. In particular, these blueprints suggest the structures of the junction molecules that may be used as basic building blocks for the self-assembly of those cages along the lines of [15, 16].

Acknowledgements

AT has been supported by an EPSRC Springboard Fellowship, and RT by an EPSRC Advanced Research Fellowship. RT moreover gratefully acknowledges funding for NEG via a Research Leadership Award of the Leverhulme Trust.

References

- [1] L. Tang, K. N. Johnson, L. A. Ball, T. Lin, M. Yeager, J. E. Johnson, The structure of pariacoto virus reveals a dodecahedral cage of duplex RNA, *Nat Struct Biol* 8 (1) (2001) 77–83.
- [2] K. Toropova, G. Basnak, R. Twarock, P. G. Stockley, N. A. Ranson, The three-dimensional structure of genomic RNA in bacteriophage MS2: implications for assembly, *J Mol Biol* 375 (3) (2008) 824–36.
- [3] S. H. E. van den Worm, R. I. Koning, H. J. Warmenhoven, H. K. Koerten, J. van Duin, Cryo electron microscopy reconstructions of the leviviridae unveil the densest icosahedral RNA packing possible, *J Mol Biol* 363 (4) (2006) 858–65.
- [4] J. H. Chen, N. C. Seeman, Synthesis from DNA of a molecule with the connectivity of a cube, *Nature* 350 (6319) (1991) 631–3.

- [5] R. P. Goodman, I. A. T. Schaap, C. F. Tardin, C. M. Erben, R. M. Berry, C. F. Schmidt, A. J. Turberfield, Rapid chiral assembly of rigid DNA building blocks for molecular nanofabrication, *Science* 310 (5754) (2005) 1661–5.
- [6] W. M. Shih, J. D. Quispe, G. F. Joyce, A 1.7-kilobase single-stranded DNA that folds into a nanoscale octahedron, *Nature* 427 (6975) (2004) 618–21.
- [7] Y. Zhang, N. C. Seeman, Construction of a DNA-truncated octahedron, *Journal of the American Chemical Society* 116 (5) (1994) 1661–1669.
- [8] G. Destito, P. Singh, K. J. Koudelka, M. Manchester, Assembling viral nanoparticles for vascular imaging and tumor-specific targeting, in: *Foundations of Nanoscience, Self-Assembled Architectures and Devices, Proceedings of FNANO07, 2007*, pp. 2–4.
- [9] J. Rudnick, R. Bruinsma, Icosahedral packing of RNA viral genomes, *Phys Rev Lett* 94 (3) (2005) 038101–038105.
- [10] N. Jonoska, R. Twarock, Blueprints for dodecahedral DNA cages, *Journal of Physics A: Mathematical and Theoretical* 41 (30) (2008) 304043–304057.
- [11] N. Jonoska, M. Saito, Boundary components of thickened graphs, in: *DNA7: Revised Papers from the 7th International Workshop on DNA-Based Computers*, Springer-Verlag, London, UK, 2002, pp. 70–81.
- [12] M. J. Greenberg, J. R. Harper, *Algebraic Topology*, The Benjamin/Cummings Publishing Comp., 1981.
- [13] P. S. Ho, B. F. Eichman, The crystal structures of DNA holliday junctions, *Curr Opin Struct Biol* 11 (3) (2001) 302–8.
- [14] P. W. K. Rothemund, Folding DNA to create nanoscale shapes and patterns, *Nature* 440 (7082) (2006) 297–302.
- [15] P. Sa-Ardyen, N. Jonoska, N. C. Seeman, Self-assembly of irregular graphs whose edges are DNA helix axes, *J Am Chem Soc* 126 (21) (2004) 6648–57.
- [16] P. Sa-Ardyen, N. Jonoska, N. C. Seeman, Self-assembling DNA graphs, in: *DNA8: Revised Papers from the 8th International Workshop on DNA Based Computers*, Springer-Verlag, London, UK, 2003, pp. 1–9.